Solvent-Induced Novel Morphologies in Diblock Copolymer Blend Thin Films

Yongzhong Chen, Zongbao Wang, Yumei Gong, Haiying Huang, and Tianbai He*

State Key Laboratory of Polymer Physics and Chemistry, Changchun Institute of Applied Chemistry, Graduate School of the Chinese Academy of Sciences, Changchun, Jilin 130022, People's Republic of China

Received: August 1, 2005; In Final Form: December 11, 2005

We report the morphology and phase behaviors of blend thin films containing two polystyrene-*b*-poly(methyl methacrylate) (PS-*b*-PMMA) diblock copolymers with different blending compositions induced by a selective solvent for the PMMA block, which were studied by transmission electron microscopy (TEM). The neat asymmetric PS-*b*-PMMA diblock copolymers employed in this study, respectively coded as $\mathbf{a}_1$ and $\mathbf{a}_2$, have similar molecular weights but different volume fractions of PS block ($f_{PS} = 0.273$ and 0.722). Another symmetric PS-*b*-PMMA diblock copolymer, coded as **s**, which has a PS block length similar to that of $\mathbf{a}_1$, was also used. For the asymmetric $\mathbf{a}_1/\mathbf{a}_2$ blend thin films, circular multilayered structures were formed. For the asymmetric $\mathbf{a}_1$/symmetric **s** blend thin films, inverted phases with PMMA as the dispersed domains were observed, when the weight fraction of **s** was less than 50%. The origins of the morphology formation in the blend thin films via solvent treatment are discussed. Combined with the theoretical prediction by Birshtein et al. (*Polymer* **1992**, *33*, 2750), we interpret the formation of these special microstructures as due to the packing frustration induced by the difference in block lengths and the preferential interactions between the solvent and PMMA block. Results obtained here suggest that diblock copolymer blend thin films treated with a selective solvent offer an alternative and attractive approach to control the self-organization of polymers.

Introduction

The self-organization of materials is a significant field for its application in the creation of various sized structures.[1] Competing interactions including hydrophobic and hydrophilic effects, hydrogen bonding, electrostatic interactions, and van der Waals forces have been employed to achieve structural order over many length scales.[2] Among those self-assembling materials, block copolymers have played a prominent role in nanoscience and nanotechnology.[3−6] Some reviews have summarized various methods to control block copolymer microdomain structures and routes to the fabrication of nanomaterials by use of self-assembled copolymers.[7−9]

As is known, the phase behavior of diblock copolymers can be controlled by synthesizing precisely tailored diblock copolymers. Another route to control block copolymer morphologies is through polymer blending, in which two or more block copolymers with different morphologies are mixed together to get a desired morphology.[10−18] Furthermore, blending of diblock copolymers affords the potential to form new phase morphologies that may not be found in neat diblock copolymers. Some complex morphologies such as gyroid structures are also obtained in binary blends of diblock copolymers.[12,15] Efforts have focused on the structures of block copolymer mixtures in bulk. However, only relatively few reports have paid attention to block copolymer blend thin films.[19,20] The control of microstructures of block copolymer thin films is very crucial not only in their physics but also in their applications in nanotechnology. Generally, interfacial energies[21−24] and commensurability[25,26] determine the phase behavior of block copolymer thin films. Thus, changing interfacial energies is a common approach to prepare block copolymer thin films with perfectly ordered domains, and this way is usually combined with electric fields which are used to overcome interfacial interactions to orient nanoscopic domains within diblock copolymer films.[26−29] Chemically heterogeneous substrates are employed to control nanoscale surface interactions and subsequent macromolecular ordering.[30,31] In addition, graphoepitaxy is another effective way to induce long-range order in block copolymer thin films.[32] These routes to produce ordering in block copolymer thin films need thermal treatment. Recently, other nonequilibrium ways have been noted. For instance, solvent-influenced ordering has been exploited to control the microstructures of block copolymer thin films without any thermal treatment.[33−36] Another route is the adsorption of diblock copolymers from a selective solvent onto a flat solid substrate resulting in the formation of laterally ordered microdomains.[37−40] Combined with the solvent-annealing approach and micelle adsorption, we have introduced selective solvents to induce ordering in polystyrene-*b*-poly(methyl methacrylate) (PS-*b*-PMMA) diblock copolymer films.[41]

In this work, we extend the solvent treatment means to the self-organization of PS-*b*-PMMA diblock copolymer blends within thin films. We investigated the phase behavior of asymmetric/asymmetric and asymmetric/symmetric PS-*b*-PMMA binary blend systems in thin films that were treated with PMMA-selective solvent vapor. Likewise, the chain packing effects induced by the junctions of the diblocks anchored to the same interface[15,42,43] also exist in diblock copolymer thin film mixtures treated by the selective solvents. Due to the selectivity of the solvent, the phase behavior of diblock copolymer blend films/solvent systems may exhibit uniquely from that of thermally treated diblock mixtures. It should be emphasized that the circular multilayered structures were obtained in PS-*b*-PMMA blend thin films via solvent treatment. The multilayered cylindrical morphology was predicted for blends of diblock copolymers $A-B_1$ and $A-B_2$,

* Corresponding author. E-mail: tbhe@ciac.jl.cn.

10.1021/jp054260k CCC: $33.50
Published on Web 01/07/2006

TABLE 1: Characteristics of PS-*b*-PMMA Diblocks

code	$M_{n,PS}-M_{n,PMMA}$[a] $\times 10^{-3}$	N[b]	w_{PS}[c]	f_{PS}[d]	M_w/M_n
$\mathbf{a}_1$	47.4−140.4	1860	0.252	0.273	1.11
s	50−54	1021	0.486	0.513	1.04
$\mathbf{a}_2$	140−60	1946	0.70	0.722	1.10

[a] $M_{n,k}$, number-average molecular weight of the PS or PMMA. [b] N, total number-average degree of polymerization of the diblock. [c] w_{PS}, PS weight fraction. [d] f_{PS}, volume fraction of the PS block calculated from $f_{PS} = (w_{PS}/\rho_{PS})/(w_{PS}/\rho_{PS} + (1 - w_{PS})/\rho_{PMMA})$ by using the following densities for the PS and PMMA blocks: $\rho_{PS} = 1.05$ g cm^{-3} and $\rho_{PMMA} = 1.17$ g cm^{-3}.

TABLE 2: Characteristics of the Blend Films $\mathbf{a}_1/\mathbf{a}_2$ and $\mathbf{a}_1$/s

$w_{\mathbf{a}_1}/w_{\mathbf{a}_2}$[a]	Φ_{PS}[b]	$\Phi_{\mathbf{a}_1}$[c]	$w_{\mathbf{a}_1}/w_{\mathbf{s}}$[a]	Φ_{PS}[b]	$\Phi_{\mathbf{a}_1}$[c]
50/50	0.503	0.489	86/14	0.308	0.854
33/67	0.577	0.322	75/25	0.329	0.745
67/33	0.428	0.655	67/33	0.354	0.661
			50/50	0.393	0.488
			33/67	0.434	0.327

[a] $w_{\mathbf{a}_1}/w_{\mathbf{a}_2}$ and $w_{\mathbf{a}_1}/w_{\mathbf{s}}$, weight fraction ratio in the blend. [b] Φ_{PS}, volume fraction of PS in the blend. [c] $\Phi_{\mathbf{a}_1}$, volume fraction of $\mathbf{a}_1$ in the blend.

where the A block was the same length for both copolymers.[44] However, to date, this theoretical prediction has not been realized in the thermoequilibrium state. In this paper, we show that multilayered microphase structures can be gained in diblock copolymer blends by use of a selective solvent. Our method to control the self-assembly of diblock copolymer mixtures by a selective solvent could be an effective way to generate new types of ordered structures of polymers.

Experimental Section

Asymmetric and symmetric PS-*b*-PMMA diblock copolymers were purchased from Polymer Source Inc. and used as received. Table 1 gives the characteristics of the copolymers used in this study. Two asymmetric diblocks coded as $\mathbf{a}_1$ and $\mathbf{a}_2$, and one symmetric diblock coded as **s**, have been used. $\mathbf{a}_1$ and $\mathbf{a}_2$ have similar molecular weights, with opposite signs of their spontaneous curvature. $\mathbf{a}_1$ and **s** have similar lengths of PS block and different lengths of PMMA block.

Two sets of binary diblock copolymer blends, one asymmetric/asymmetric diblock copolymer blend $\mathbf{a}_1/\mathbf{a}_2$, and another asymmetric/symmetric $\mathbf{a}_1$/**s**, were prepared. The binary mixtures of diblocks were dissolved in toluene, forming 5 mg/mL solutions of the block copolymers in toluene. The composition of each blend is shown in Table 2. Thin blend films were prepared on carbon-coated mica spun cast at 3000 rpm from their solutions for 40 s. The films were then put in an airtight vessel with ca. 31 cm^3 volume with 100 μL of the reservoir acetone at the initiation of the solvent-annealing process. After being exposed for different times to an acetone vapor, the samples were removed from the vessel quickly and air-dried at room temperature (ca. 18.5−20 °C). The film thickness measure was conducted by means of atomic force microscopy (AFM) using a Nanoscope IIIa (Digital Instruments Inc., Santa Barbara, CA). The initial film thicknesses were determined from bearing analysis in which a sharp metal razor blade was used to scratch a copolymer film but not the underlying Si substrates. Because carbon-coated mica substrates are easily damaged by a hard blade, the films used in thickness measurement were spin-coated onto silicon wafers. The average thickness of each film determined in this fashion was about 40 nm. Acetone is a good solvent for PMMA and a nonsolvent for PS, which has been confirmed by comparing the polymer−solvent interaction parameters between the two blocks, PS and PMMA.[41]

Transmission electron microscopy (TEM) was conducted in a JEOL 1011 TEM with an accelerating voltage of 100 kV in the bright-field mode. For the TEM studies, carbon-coated mica substrates were used; the film and its carbon support were floated off onto a pool of deionized water and picked up with copper mesh TEM grids. Specimens used for TEM observation were exposed to RuO_4 vapor for 2 h, which selectively stains the PS block and provides contrast in electron density. After RuO_4 staining, dark regions of the bright-field TEM images are identifiable with the PS domains whereas the bright regions are PMMA.

Results and Discussion

This section is divided into two parts. The first part presents the morphology study of asymmetric/asymmetric $\mathbf{a}_1/\mathbf{a}_2$ blend thin films treated with acetone vapor. The second part describes the morphologies of asymmetric/symmetric $\mathbf{a}_1$/**s** blend thin films. Each part discusses the effects of the chain lengths and solvent−polymer interactions on the production of the phase structures in the blend thin films.

Morphology of $\mathbf{a}_1/\mathbf{a}_2$ Binary Blend Thin Films. The compositions of the mixtures are shown in Table 2. The neat PS-*b*-PMMA copolymers employed here have alike molecular weights but different volume fractions of PS. Under solvent conditions, the morphology of the thin films is time dependent, and the equilibrium state is determined with difficulty. Here, we do not give a complete time scope of the evolution of morphologies in PS-*b*-PMMA diblock copolymer blend thin films, but only present the microstructures of thin films obtained by short-time annealing treatment. The $\mathbf{a}_1/\mathbf{a}_2$ blend thin films were annealed in acetone vapor at ca. 18.5 °C.

Figure 1 gives TEM images of $\mathbf{a}_1/\mathbf{a}_2$ 50/50 thin film treated by acetone vapor. The 1 h preparation resulted in a spherical morphology with PS block as the dispersed phases. In Figure 1a, one can see that the size of the PS domains is not very uniform: the largest PS domain diameter is about 75.4 nm and the smallest is about 40 nm. The distribution of the PS domain sizes may be induced by the different fractions of the PS block of the two components in the microdomains. That is, the larger PS domains mean higher contents of longer PS chains of $\mathbf{a}_2$ in the domains. Treatment of 6.5 h disrupted the structures, as shown in Figure 1b. There exist two types of morphologies. One is a simple PS ring, and the other is a triple coaxial circular microdomain structure with PS as the dark core, PMMA as the bright shell, and PS as the dark ring. For the triple coaxial circular domains, the diameter of the PS core is ∼36 nm, and the spacing of the adjacent coaxial domains is ∼115 nm. The PS rings disperse among the core−shell multilayered domains, which form the dot-free defects of the 6-fold symmetric

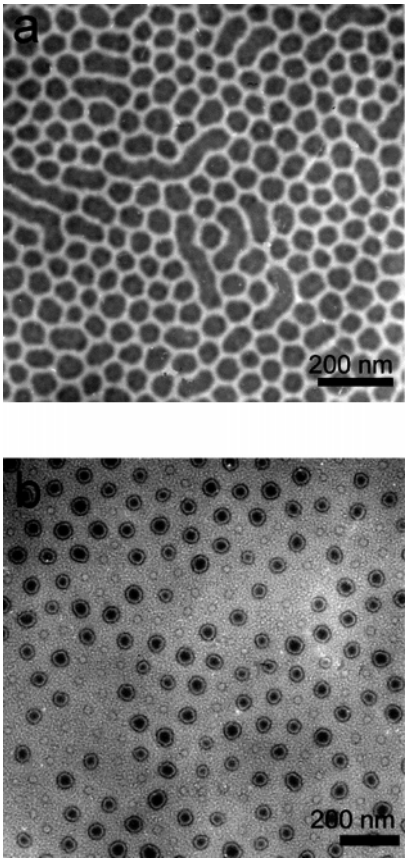

Figure 1. TEM micrographs of $\mathbf{a}_1/\mathbf{a}_2$ 50/50 blend thin films annealed in acetone vapor at 18.5 °C respectively for (a) 1 and (b) 6.5 h.

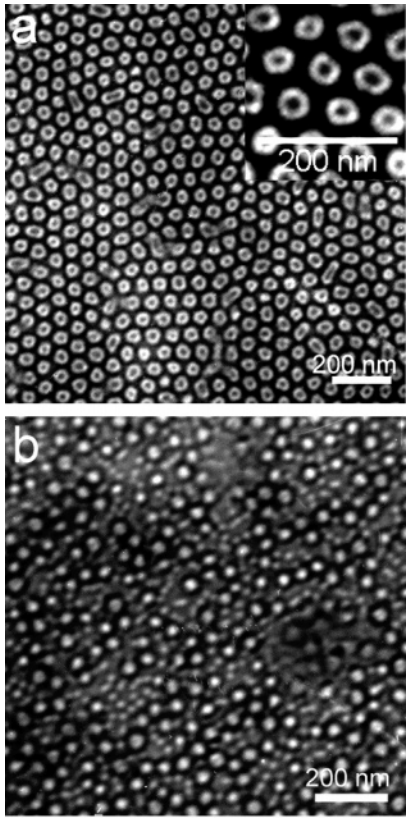

Figure 2. TEM micrographs of $\mathbf{a}_1/\mathbf{a}_2$ 67/33 blend thin films annealed in acetone vapor at 18.5 °C respectively for (a) 1 and (b) 6.5 h. The inset to (a) is a local magnification image.

multilayered domains. These PS rings should be related to the separation of $\mathbf{a}_1$ and $\mathbf{a}_2$ diblock copolymers.

Figure 2 shows TEM micrographs of the microstructures of $\mathbf{a}_1/\mathbf{a}_2$ 67/33 thin films induced by acetone vapor. Figure 2a clearly displays the formation of hexagonal packed circular multilayered microdomains. The average spacing of the adjacent domains is ∼74 nm, shown in Figure 2a. The diameter of the PS forming cores is ∼21 nm. The periphery of the cores appears bright, suggesting that the PMMA block forms layerlike domains around the PS cores. The thickness of the PMMA layers is ∼15.7 nm. The outsides of the PMMA layers appear dark, indicating that the matrix is the PS microphase. The PS cores and PMMA layers are coaxial, forming two layered domains with circular shape packed in a hexagonal array in the PS microphase. The inset of Figure 2a clearly indicates a three-phase double coaxial circular microdomain morphology. This result shows that a three-phase morphology, which is usually gained in ABC triblock copolymers,[35] may be realized by blending diblock copolymers. The PS volume fraction in the double cylinders is ∼0.578, which is larger than that (0.428) in the blend. This can be attributed to the interactions between the substrate and the blocks of PS-*b*-PMMA. The PMMA component resides at the carbon substrate.[45] For the $\mathbf{a}_1/\mathbf{a}_2$ 67/33 thin film, because of the relatively high fraction of $\mathbf{a}_1$ compared to $\mathbf{a}_2$, the PMMA component residing at the substrate may mainly consist of the PMMA block of $\mathbf{a}_1$. Thus, the fraction of $\mathbf{a}_1$ in the core−shell domains is decreased, which leads to the increase of the PS fraction in the multilayered domains. With the annealing time increased to 6.5 h, these structures were transformed into disordered arrays of spherical microdomains, as shown in Figure 2b. It should be noted that, here, the core of the domains is PMMA, and the corona is PS. These circular domains should be formed by the dividing of the multilayered domains, as shown in Figure 2a. It is difficult to realize domains with narrow distribution in the process of producing spherical morphology from the multilayered domains, so only disordered patterns were formed as shown in Figure 2b.

Parts a and b of Figure 3 represent TEM images of the thin film mixtures $\mathbf{a}_1/\mathbf{a}_2$ 33/67 annealed by acetone respectively for 1 and 6.5 h. Figure 3a displays an in-plane core−shell cylindrical structure with PS as the core and PMMA as the shell. The lateral spacing between core−shell cylinders in Figure 3a is ∼70 nm. The PS core should be formed by the PS block of $\mathbf{a}_1$, and the shell should be the stacking of the PMMA chains of both $\mathbf{a}_1$ and $\mathbf{a}_2$. This is attributed to the different PMMA volume fractions of $\mathbf{a}_1$ and $\mathbf{a}_2$. The PS block of $\mathbf{a}_1$ is inclined to form the core because of the higher PMMA fraction than that of $\mathbf{a}_2$. Further treatment resulted in the formation of circular multilayered microdomains, as shown by Figure 3b. The cores of the domains are formed by PS. The average diameter of the PS cores is ca. 23 nm, determined from Figure 3b. The layerlike domains around the PS cores are formed by PMMA. The thickness of the PMMA layers is ca. 16 nm, which is similar to that shown in Figure 2a. Around the PMMA layers are PS shells. The PS, PMMA, and PS microphases form triple coaxial domains with a circular shape packed in a hexagonal array in the PMMA phase, which forms the matrix. Therefore, Figure 3b shows a four-phase triple coaxial circular microdomain structure. The dispersed domains can be divided into three parts: PS core, PMMA middle layer, and PS shell with thickness of ∼11.9 nm, from the inner to the exterior of each domain. The spacing of the adjacent domains in Figure 3b is ca. 87 nm. The PS volume fraction is ∼0.484, which is lower than that (0.577) in the blend. In this situation, the PMMA component lying on the substrate can mainly consist of the PMMA block

Figure 3. TEM micrographs of $\mathbf{a}_1/\mathbf{a}_2$ 33/67 blend thin films annealed in acetone vapor at 18.5 °C respectively for (a) 1 and (b) 6.5 h and annealed in a vacuum (c) at 165 °C for 24 h. The inset to (b) is a local magnification image.

of $\mathbf{a}_2$, which increased the PS fraction in the multilayered domains. The multilayered domains in Figure 3b should be formed from the dividing of in-plane core−shell cylinders in Figure 3a. For comparing the solvent-induced microphase separation with that by thermal treatment, we observed the microstructure of the thin film annealed in a vacuum at 165 °C for 24 h, which is shown in Figure 3c. In this situation, a striped surface morphology was obtained. The PMMA and PS blocks formed short stripes without long ordering. In local regions there exist PMMA dot domains which are embedded in the PS matrix. Obviously, from the results of Figure 3 one can conclude that the solvent has great effect on the formation of the multilayered domains. Due to the asymmetric interactions between the solvent and the components of PS-*b*-PMMA, the blend thin films treated with acetone show unique phase behaviors different from those obtained by thermal treatment.

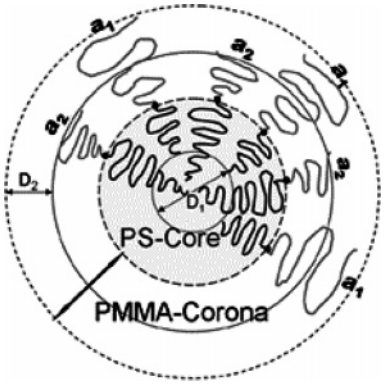

Figure 4. Schematic illustration of packing frustration induced by the difference between the polymer chain lengths assuming the chemical junctions of $\mathbf{a}_1$ and $\mathbf{a}_2$ segregating on the same interface. The black chains represent PS, and the gray chains represent PMMA.

The following part discusses the formation of the special structures in the $\mathbf{a}_1/\mathbf{a}_2$ blend thin films. At first, we assume that the chemical junctions of $\mathbf{a}_1$ and $\mathbf{a}_2$ segregate on the same interface when the microphase separation happens, as illustrated by Figure 4. The PS chains form the cores of the domains, and the PMMA chains form the corona. Because of the different lengths of PS and PMMA chains between these two components, there is a zone labeled D_1 in the core with lower PS chain packing density caused by the differences in PS chain lengths. Likewise, there is a region D_2 with lower chain packing density in the corona regions caused by the differences in PMMA chain lengths. This chain packing frustration is produced by the distribution of the chain lengths within the blend.[12,43] For eliminating this density frustration, the chains of $\mathbf{a}_1$ and $\mathbf{a}_2$ may stack by means of other ways.

Noolandi and Hashimoto et al. have reported the case of blending of a long diblock and a short diblock, indicating that the packing frustration can be relieved by modifying interface curvatures.[11,17,43] Koneripalli et al. have also studied phase behavior of blends of asymmetric diblock copolymers having similar molecular weights and different volume fractions.[20] They reported that a lamellar morphology was formed even when the individual components exhibit a nonlamellar morphology in the pure melt state. It should be noted that these morphologies are obtained by thermal treatment. However, when a selective solvent is used to induce microphase separation in a blend film of diblock copolymers, the manner of relieving packing frustration may be not similar to those of thermotropic phase transitions.

In the case of blends of $\mathbf{a}_1/\mathbf{a}_2$ annealed by acetone, because of the strong solvent affinity for PMMA, PMMA chains are swollen by the solvent, which increases the effective volume of PMMA chains. Thus, the interfaces of the domains prefer bending to the PS phase. It is difficult to form a lamellar morphology in the $\mathbf{a}_1/\mathbf{a}_2$ blend films induced by acetone. Then, the self-assembly of polymer chains happened at a bending interface, which resulted in multilayered structures shown in Figures 2a and 3b. Figure 5shows two typical multilayered microstructures illustrated by the experimental results shown in Figures 2a and 3b. The formation of these special structures resulted from packing frustration of both PS and PMMA chains. As illustrated in Figure 5, chemical junctions of $\mathbf{a}_1$ and $\mathbf{a}_2$ segregate on different interfaces, and then generate microdomains with multiple interfaces. Figure 5a displays a three-phase structure, which shows the morphology shown in Figure 2a. The inner is the core of the domain formed by PS, which is surrounded by a PMMA layer. Due to the lower PS volume

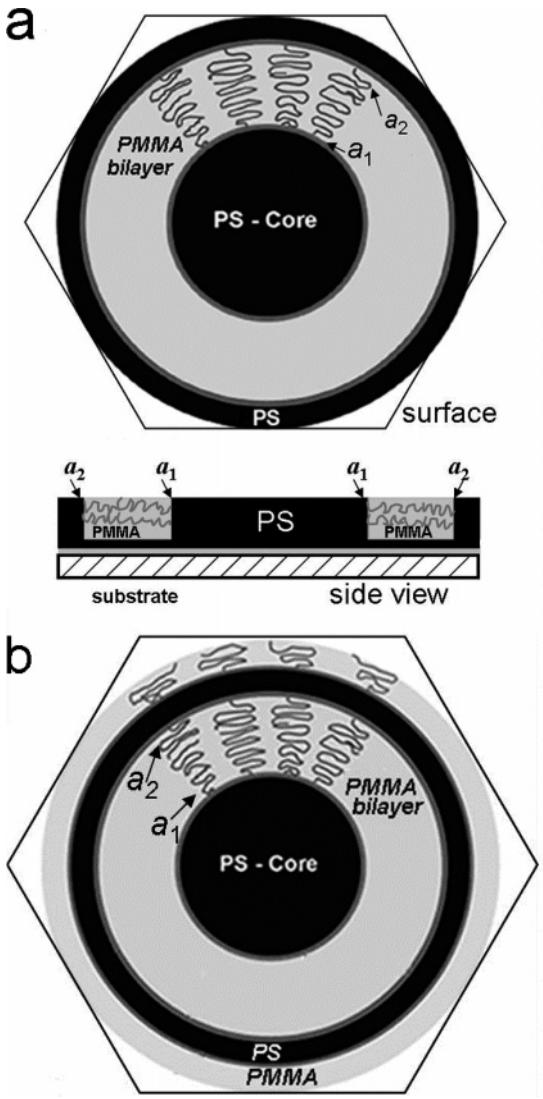

Figure 5. Schematic illustrations of two possible morphologies of $\mathbf{a}_1$/$\mathbf{a}_2$ blend thin films.

fraction of $\mathbf{a}_1$ compared to that of $\mathbf{a}_2$, the curvature of the $\mathbf{a}_1$ chain should be larger than that of the $\mathbf{a}_2$ chain in the presence of acetone. It can be concluded that the core of the domains consists of the PS block of $\mathbf{a}_1$. The PMMA shell is a bilayer structure formed via stacking of the PMMA chains of $\mathbf{a}_1$ and $\mathbf{a}_2$. From Figure 5, one can see that the polymer chains self-assembled along the direction normal to the PS−PMMA interfaces. The PS cores and PMMA bilayers form the dispersed domains packed in a hexagonal array in the PS matrix. Thus, the morphology in Figure 5a is a three-phase structure. Figure 5a also gives a side view, which illustrates a possible sectional structure of the thin film. For the preferential interactions between the PMMA block and the substrate, a PMMA layer should be formed on the substrate surface. Thus, the core−shell domains reside on the sublayer consisting of PS and PMMA. However, the free surface may not be completely covered by the PS block, when the thin film is exposed to acetone vapor. Because of the preferential interactions between PMMA and acetone, the PS and PMMA components should coexist on the surface of the film.[46]

For further reviewing the origins of the above morphologies, it is essential to estimate the free energy of the blend systems. The equilibrium free energy $Q_{CC'}$ of the multilayered structure (double cylinder) has been given by Birshtein et al.:[44]

$$Q_{CC'} = \left[(1-q)Q_{C_0} + qQ_{C'_0}\frac{r_{10}^2}{r_{20}^2}\right]^{1/3}\left[(1-q)Q_{C_0} + qQ_{C'_0}\frac{r_{10}}{r_{20}}\right]^{2/3} \quad (1)$$

In the case of Figure 5, q is the number fraction of $\mathbf{a}_2$. Q_{C_0}, $Q_{C'_0}$, r_{10}, and r_{20} are given by eqs 8, 28, 31, and 32 in ref 44. According to the calculations of eq 1 and ref 44, at mean mixture composition near 75−85% PS block the multilayered structure should be the most stable. However, in the case of this paper, the multilayered structure was realized although the PS fractions are only near 50%. Therefore, the selective solvent has played an important role in forming the multilayered structure. The solvent acetone can effectively decrease the chain tangles of PMMA and make the PMMA chains of the blend components able to stack along the same direction, leading to the formation of the multilayered domains.

In addition, in the PMMA bilayer the driving powers of the packing of the polymer chains are weak van der Waals forces. These structures lack enough stability. For example, as shown in Figure 2b, the multilayered structures can be transformed to disordered micellar structures. The distribution of the PS and PMMA chains in the arrays displayed by Figure 2b is disordered. The microdomains with diverse dimensions arrange together without order. This can be also a way of decreasing packing frustration.

The three-layer structure illustrated by Figure 5b represents the experimental result revealed by Figure 3b. The cores of the domains are still composed of the PS block of $\mathbf{a}_1$, which are enveloped by the PMMA layers. The PMMA layers are surrounded by the PS shells. In this situation, the matrix is formed by PMMA, and the PMMA sandwich is also a bilayer structure formed by the packing of the PMMA blocks of $\mathbf{a}_1$ and $\mathbf{a}_2$, which is similar to that shown in Figure 5a. The PMMA sandwich has a thickness near that displayed in Figure 5a. The dispersed domains as shown by Figure 5b are comprised of three parts: PS cores, PMMA middle bilayers, and PS shells. These dispersed domains combined with the PMMA matrix form a four-phase structure, which is very similar to that obtained in the tetrablock quaterpolymer reported by Hasegawa et al.[48] Integrating the above analysis, the multilayered structure in $\mathbf{a}_1$/$\mathbf{a}_2$ blend films consists of two parts: one is the inner domain formed by $\mathbf{a}_1$, and the other is the outer layer engendered by $\mathbf{a}_2$. The difference between the two morphologies in Figure 5 is that the components of the outsides of the dispersed domains are different, depending on the weight fraction of $\mathbf{a}_1$ or $\mathbf{a}_2$ in the blends. Comparing Figures 4 and 5, we can find that the density frustration illustrated in Figure 5 is lower than that in Figure 4. Thus, the morphologies shown in Figure 5 can be obtained under certain conditions.

The above experimental results show that the three- or four-phase structure usually found in multiblock copolymers can be obtained in diblock copolymer blend films treated with a selective solvent. The blends also avoid complex synthesis of multiblock copolymers. Further, we noted that the core−shell cylinder morphology has also been gained even in a neat diblock copolymer,[47] but it is rarely found in most diblock copolymers or in blends of diblocks. Therefore, the method to construct the core−shell morphology in diblock copolymer blends is still essential.

In addition, it should be emphasized that the structures displayed by Figure 5 are not the unique framework of the chain arrangement in the presence of solvent. For example, some other microstructures are also realized as revealed in Figures 2 and 3, such as striped and disordered patterns.

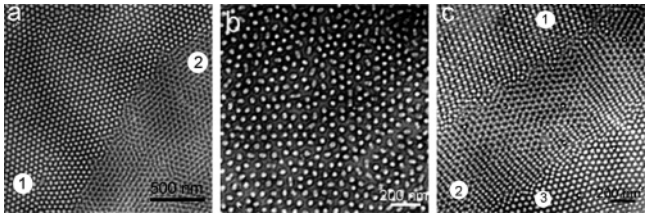

Figure 6. TEM micrographs of $\mathbf{a}_1$/**s** 75/25 blend thin films annealed in acetone vapor at 20 °C respectively for (a) 1, (b) 3, and (c) 6.5 h.

Morphology of $\mathbf{a}_1$/s Binary Blend Thin Films. The compositions of the $\mathbf{a}_1$/**s** mixtures are shown in Table 2. The two diblocks share the same length of PS block. At first, we investigated the phase behavior of $\mathbf{a}_1$/**s** 75/25 blend thin film annealed at 20 °C in acetone vapor for 1 h, as shown in Figure 6. In Figure 6a, there are obviously two regions. In region 1, the spherical PMMA microdomains as the dispersed phase arrange hexagonally in the matrix of PS. In region 2, the dispersed phases turned to PS, and the dispersed PS domains are also hexagonally packed. The average diameter of the PS domains is ∼30 nm, determined from Figure 6a. Because acetone is the preferential solvent for the PMMA block, it can increase the effective volume fraction of the PMMA block by swelling it. Thereupon, when a PS-*b*-PMMA diblock copolymer is treated by acetone, the insoluble PS block is inclined to aggregate and form the dispersed phase, and the soluble PMMA block forms the continuous phase. The structures of PS-*b*-PMMA diblock copolymer thin films obtained by acetone annealing are a kind of micellar structure. Accordingly, the PS forming dispersed phase is noted as normal phase and the PMMA forming dispersed phase is noted as inverted phase according to the selectivity of acetone for different blocks of the diblock copolymer. It can be clearly seen that the morphology of region 1 in Figure 6a is the inverted phase and that of region 2 is the normal phase. Moreover, the lateral period of the normal phases is ∼51 nm, and that of the inverted phases is ∼49 nm, shown in Figure 6a. Under other conditions, we also observed the formation of the inverted phases shown in Figure 6b,c. The coexisting normal and inverted phases are also found in the 6.5 h preparation shown in Figure 6c, in which regions 1 and 3 indicate the inverted phases and region 2 shows the normal phases.

To find whether the inverted phases could be formed at other temperatures, we observed phase behavior in $\mathbf{a}_1$/**s** 75/25 thin film mixture treated by acetone at 18.5 °C. Figure 7a shows a TEM micrograph of $\mathbf{a}_1$/**s** 75/25 thin film mixture annealed in acetone vapor for 1 h. It clearly indicates the formation of inverted phases. The dispersed PMMA microdomains exhibit hexagonal packing arrays. The average diameter of PS domains is ∼31 nm, and the spacing of the adjacent PS domains is ∼52 nm. The spacing of the adjacent PMMA domains is ∼55 nm measured by Figure 7a. When the thin film was treated for 6.5 h, PS domains with 3-fold symmetry were formed, as shown in Figure 7b. When continuous PS domains in Figure 7a separated, they formed nearly dispersed domains which arranged into hexagonal shapes. The morphology in Figure 7b can be considered to be an intermediate phase structure between the normal and inverted phases. At the same time, the size of the PS domains shown in Figure 7b is smaller than that of PS domains in normal phases.

The above-mentioned experimental results demonstrate that the morphologies of the $\mathbf{a}_1$/**s** blend films obtained at different temperatures are similar. The morphologies studied in the following $\mathbf{a}_1$/**s** blend films with various weight fraction ratios were all obtained at 18.5 °C.

Increasing the weight fraction of the asymmetric diblock $\mathbf{a}_1$, we observed the phase behavior in $\mathbf{a}_1$/**s** 86/14 blend thin films annealed in acetone vapor respectively for 1 and 6.5 h, as shown in TEM images in Figure 7c,d. Figure 7c clearly shows an inverted phase structure with two-dimensional hexagonal packed PMMA domains exhibiting approximate 6-fold symmetry. A 3-fold symmetry of PS domains is also gained, displayed in Figure 7d. Likewise, the morphology in Figure 7d can be considered as an intermediate phase structure between the normal and inverted phases.

Parts e and f of Figure 7 display TEM images of $\mathbf{a}_1$/**s** 67/33 blend thin films treated by acetone for 1 and 6.5 h. When the annealing time is 1 h, only dispersed hexagonal close packing PS domains were obtained, or only normal phases were gained. The diameter of the PS domains is ∼31 nm, and the lateral period is ∼52 nm, determined by Figure 7e. When the annealing time is 6.5 h, 6-fold packed PS domains and quasi-3-fold PS domains are formed as shown in Figure 7f. This indicates that the normal phase in Figure 7e has not reached the real stable state. Longer time treatment may disrupt this normal phase microstructure, and result in coexisting structures of 6-fold packed PS domains and quasi-3-fold PS domains.

Parts g and h of Figure 7 show TEM images of $\mathbf{a}_1$/**s** 50/50 blend thin films as the weight fraction of symmetric **s** increases from 33 to 50 wt %. Figure 7g shows a bicontinuous morphology. The PS domains connected in short ranges. Figure 7h shows a normal phase with PS as the dispersed microphases. The diameter of the PS domains is ∼36 nm, and the average distance between the adjacent PS domains is ∼58 nm, determined by Figure 7h. At this composition, we have not observed the production of the inverted phases.

When the weight ratio of $\mathbf{a}_1$ to **s** reaches 33/67, morphologies as shown in Figure 7i,j are formed. At this time, the inverted phases have not appeared. Thus, by above experimental observation, one can find that, when increasing the weight fraction of the symmetric **s** in the blends, the probability of generating inverted phases decreases.

The above results demonstrate that the inverted structure can be formed by regulating the weight fraction of the blend composition. When a neat PS-*b*-PMMA thin film is annealed by acetone, which has strong affinity for the PMMA, the PMMA blocks are inclined to form continuous microdomains, even in a diblock with PMMA as the minority composition. Under this condition in the presence of a selective solvent, this structure should be more stable thermodynamically. However, when the systems turn into diblock copolymer blends, the situation is sometimes not the case. The inverted phase with dispersive PMMA domains may be in favor of the stability of the systems under certain conditions.

Another question is that of why multilayered structures such as those in $\mathbf{a}_1$/$\mathbf{a}_2$ blends are not observed in the $\mathbf{a}_1$/**s** blend thin films. This can be interpreted from the length difference in the PS block. For $\mathbf{a}_1$/**s** blends, because the length of PS chains of $\mathbf{a}_1$ and **s** is similar, the PS chains of both diblocks are easily packed in the same space, when microphase separation happens. In this situation, the chain packing frustration is mainly due to the length variations of PMMA block. However, for $\mathbf{a}_1$/$\mathbf{a}_2$ blends, because the lengths of both PS and PMMA chains are different, it is difficult to form ordered structures when the PS or PMMA chains enter the same space. The chain packing density in $\mathbf{a}_1$/$\mathbf{a}_2$ blends is produced by differences in chain lengths of both PS and PMMA. If the PS and PMMA chains of the blends are required to form domains respectively, for relieving chain packing frustration induced by chain length

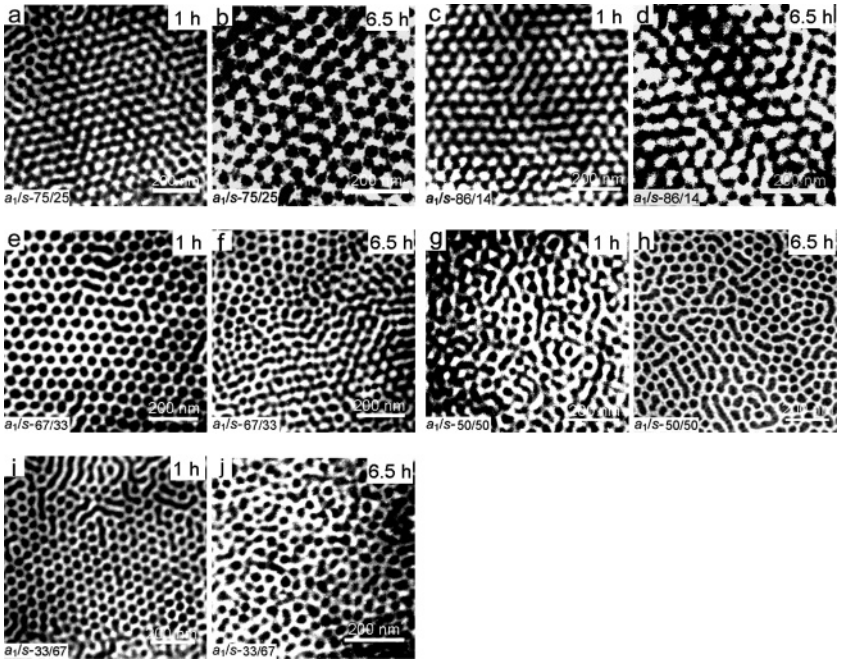

Figure 7. TEM micrographs of $\mathbf{a}_1$/**s** blend thin films annealed in acetone vapor at 18.5 °C respectively for 1 and 6.5 h. The compositions and annealing time are shown in the insets.

difference, the conformation of both PS and PMMA blocks needs to be changed. However, the preferential interactions between the PMMA block and acetone make the modification of the conformation of PMMA chains difficult. Thus, the phase behaviors of $\mathbf{a}_1$/$\mathbf{a}_2$ blend films are more complex than those of $\mathbf{a}_1$/**s**.

Reference 43 has indicated a model of blending a longer asymmetric diblock copolymer (α) and a shorter diblock (β). The addition of β to the systems α may effectively alter interface curvatures, e.g., by changing morphology from cylinders to lamellae, to realize uniform segmental density in space. In this case, the long and short polymer chains which are anchored to the interface coexist in the same microdomain space.[15,18] It should be emphasized that this situation is of thermal treatment. Consider the situation in this paper, that blend films of PS_{456}−$PMMA_{1404}$ ($\mathbf{a}_1$) and PS_{481}−$PMMA_{540}$ (**s**) are annealed by acetone. The PS chain lengths of both diblock copolymers are nearly equal, so one can conjecture that the PS block of the two diblock copolymers should enter the same space when microphase separation occurs. Figure 8illustrates two sorts of morphologies. The morphology as shown in Figure 8a is the normal phase. The chemical junctions of $\mathbf{a}_1$ and **s** are localized at the interface of the PS and PMMA domains. Because the PMMA length of **s** is shorter than that of $\mathbf{a}_1$, in the corona region, there exists a region of low packing density, denoted "LD". The chain packing density of region LD is lower than that of HD (high density), as shown in Figure 8a. This packing frustration does not favor the stability of systems for certain blend films. To keep uniform segmental density in space, interface curvatures will be changed. In the presence of selective solvents, it is difficult for the interface to adopt a geometry with a lower curvature, since this alteration needs to modify the conformation of PMMA chains. The preferential interactions between the selective solvent and PMMA block result in that the PMMA chain conformation cannot be changed greatly. Thereby, the packing frustration may be relieved by other ways, as shown in Figure 8b. Figure 8b illustrates an inverted phase structure. When the PMMA blocks form the cores of the domains, the contact of the ends of the PMMA chains increases,

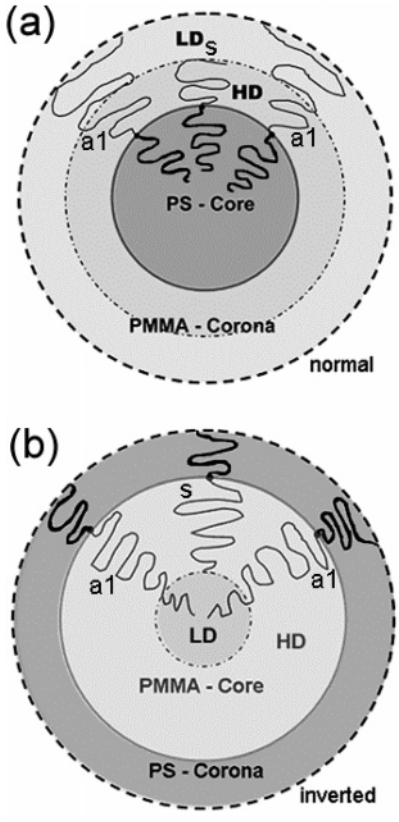

Figure 8. Schematic illustrations of normal and inverted phases in $\mathbf{a}_1$/**s** blend thin films.

as shown in region LD of Figure 8b. Thus, when the weight fraction of symmetric **s** in the blend films is lower, the chain packing frustration of inverted phases may be less than that of normal phases. Obviously, for the situation displayed in Figure 8b, the chain density in region LD is lower than that in region HD in the PMMA core. The density difference between LD and HD relates to the weight fraction of **s** in the blends. Therefore, although acetone has a strong affinity for the PMMA

block, the chain density frustration can result in the formation of inverted phase structure with PMMA as the dispersive domains in PS-*b*-PMMA blend films.

When the weight fraction of **s** in the $\mathbf{a}_1$/**s** blend films increases, the morphology of normal phase predominates; for instance, only normal phase is found in $\mathbf{a}_1$/**s** 50/50 and 33/67 blend thin films. Combined with Figure 8a, as the weight fractions of shorter **s** increase, the average distance between the ends of PMMA chains of longer $\mathbf{a}_1$ also increases; thereupon, the effective volume of region LD decreases. Therefore, when the different domains arrange together, the overlap between LD regions of different domains increases. Thus, the segmental density frustration in the corona of the domains reduces, and the resulting structure is more stable.

For further verifying the effects of solvent on the morphology formation in the $\mathbf{a}_1$/**s** blends, we compared the free energy of normal and inverted phases.

The free energy of normal phases Q_{normal} can be given by[49]

$$Q_{\text{normal}} = 3f_1^{1/3}\left[\frac{1}{4} + \frac{3}{2\pi^2}\ln(1 + f_1^{-1}) + q\frac{3}{2\pi^2}\ln\left(1 + q\frac{f_1 - f_2}{f_2(1 + f_1)}\right)\right]^{1/3} \quad (2)$$

where

$$f_1 = N_{\text{PS}}/N_{\text{PMMA(s)}}; \qquad f_2 = N_{\text{PS}}/N_{\text{PMMA}(\mathbf{a}_1)} \quad (3)$$

The free energy of inverted phases Q_{inverse} can be given by[49,50]

$$Q_{\text{inverse}} = 3\left[\frac{1}{4}(1 + \alpha q)^2 G(\alpha,q) + \frac{3}{2\pi^2}(1 + \alpha q)\ln\left(1 + \frac{f_1}{1 + \alpha q}\right)\right]^{1/3} \quad (4)$$

$$\begin{aligned} G = (1 + \alpha q)\{(u^2 - l_1^2)^{1/2}[6(1 + \alpha)u^2 + \\ 0.5l_1^2 u(1 - 5\alpha - 10\alpha^2) - 0.5l_1^2(1 + \alpha) - \\ u^3(6 - \alpha - 5\alpha^2)] + [-0.5l_1^4\alpha(1 + 5\alpha) + \\ 0.5l_1^2u^2(-10 + 3\alpha + 15\alpha^2) - 5(1 + \alpha)u^2(u^2 - l_1^2) + \\ u^4(6 - \alpha - 5\alpha^2)]\} - 3l_1^2\alpha q \end{aligned} \quad (5)$$

where l_1 is the relative thickness of the short block layer given by[49,50]

$$\frac{q}{1 + \alpha q} = \frac{[1 - l_1^2(1 - \alpha^2)]^{1/2} - \alpha}{1 - \alpha^2} - l_1^2 \ln\frac{l_1(1 - \alpha)}{1 - [1 - l_1^2(1 - \alpha^2)]^{1/2}} \quad (6)$$

$$u = \frac{2(1 + \alpha q)}{1 - \alpha^2}[1 - \alpha[1 - l_1^2(1 - \alpha^2)]^{1/2}] \quad (7)$$

$$q = n_{\mathbf{a}_1}/(n_{\mathbf{a}_1} + n_{\mathbf{s}}) \quad (8)$$

in which $n_{\mathbf{a}_1}$ and $n_{\mathbf{s}}$ are the number of molecules of $\mathbf{a}_1$ and **s**.

The relative difference in lengths of PMMA blocks is

$$\alpha = (N_{\text{PMMA}(\mathbf{a}_1)} - N_{\text{PMMA(s)}})/N_{\text{PMMA}(\mathbf{a}_1)} \quad (9)$$

According to eqs 2 and 4, in all the blend compositions of $\mathbf{a}_1$/**s** of this work, Q_{inverse} is always smaller than Q_{normal}. However, at certain compositions, only normal phases are obtained, such as the experimental results shown in Figure 7h,i. This can also be attributed to the preferential interactions between acetone and PMMA blocks that make the interfaces prefer to bend to the PS phases. The solvent effects can lead to the formation of morphologies different from those of thermoequilibrium.

For a neat PS-*b*-PMMA diblock copolymer treated by acetone, the PMMA block forms the continuous phase even though the PS block is the minority composition because of the preferential interactions between the solvent and PMMA block.[39,41] However, for the blend systems studied in this work, the case is changed. The inverted phase can be formed even though the PMMA block serves as the majority composition; e.g., the inverted phase is found in the $\mathbf{a}_1$/**s** 75/25 blend films treated by acetone, as shown in Figure 6. In this case, the inverted phase is obtained by varying the weight fraction of the blending participants. For the blend systems, the morphology depends not only on the interactions between the solvent and the blocks, but also on the differences in chain lengths.

Conclusions

In conclusion, we have observed the self-assembly of PS-*b*-PMMA diblock copolymers in their blend thin films annealed by the selective solvent acetone. Varying blended components, we have obtained novel morphologies such as inverted phase or multilayered structure in diblock copolymer binary blend thin films. The interesting microstructures in $\mathbf{a}_1$/$\mathbf{a}_2$ and $\mathbf{a}_1$/**s** blend thin films obtained in this work can be ascribed to two important factors: one is the packing frustration induced by differences in the mean PS and PMMA block lengths; the other is the preferential interactions between acetone and the PMMA block, which play an important role in the formation of morphologies in the thin films, and make the phase behaviors of the blends very different from those in thermodynamic equilibrium conditions. The process of the formation of these structures in the blend films is actually one that reduces the packing frustration by control of the self-organization of diblock copolymers according to special chain arrangements. Although acetone is a selective solvent of PMMA blocks, it can also affect the mobility of PS blocks in a ultrathin film, which has been verified in similar experiments.[39] Obviously, the solvent-induced structures in the blend thin films do not reach their thermoequilibrium state. However, as both components PS and PMMA are vitrified and stiff at room temperature, the formed structures after solvent extraction can remain stable under ambient conditions.

We believe that our method to control structures of diblock copolymer blend thin films by selective solvents provides a promising way to achieve new morphologies in polymer thin films. The phase structures obtained in this work may cover only a minor fraction of potential structures of diblock copolymer blend thins films induced by selective solvents. A thorough investigation of the assembling of block chains with different lengths is essential to better understanding of the phase behavior in the diblock copolymer blend thin films treated with solvent vapor, which will be a topic of further work.

Acknowledgment. This work was supported by the National Science Foundation of China (20234020) and the Chinese Academy of Sciences (KJCX2-SW-H07).

References and Notes

(1) Förster, S.; Plantenberg, T. *Angew. Chem., Int. Ed.* **2002**, *41*, 688.
(2) Muthukumar, M.; Ober, C. K.; Thomas, E. L. *Science* **1997**, *277*, 1225.
(3) Hamley, I. W. *The Physics of Block Copolymers*; Oxford University Press: Oxford, 1998.

(4) Park, M.; Harrison, C.; Chaikin, P. M.; Register, R. A.; Adamson, D. H. *Science* **1997**, *276*, 1401.
(5) Thurn-Albrecht, T.; Schotter, J.; Kastle, G. A.; Emley, N.; Shibauchi, T.; Krusin-Elbaum, L.; Guarini, K.; Black, C. T.; Tuominen, M. T.; Russell, T. P. *Science* **2000**, *290*, 2126.
(6) Jeong, U.; Kim, H.; Rodriguez, R. L.; Tsai, I. Y.; Stafford, C. M.; Kim, J. K.; Hawker, C. J.; Russell, T. P. *Adv. Mater.* **2002**, *14*, 274.
(7) Förster, S.; Antonietti, M. *Adv. Mater.* **1998**, *10*, 195.
(8) Lazzari, M.; López-Quintela, M. A. *Adv. Mater.* **2003**, *15*, 1583.
(9) Park, C.; Yoon, J.; Thomas, E. L. *Polymer* **2003**, *44*, 6725.
(10) Hashimoto, T.; Yamasaki, K.; Koizumi, S. *Macromolecules* **1993**, *26*, 2895.
(11) Shi, A.-C.; Noolandi, J. *Macromolecules* **1995**, *28*, 3103.
(12) Spontak, R. J.; Fung, J. C.; Braunfeld, M. B.; Sedat, J. W.; Agard, D. A.; Kane, L.; Smith, S. D.; Satkowski, M. M.; Ashraf, A.; Hajduk, D. A.; Gruner, S. M. *Macromolecules* **1996**, *29*, 4494.
(13) Kane, L.; Satkowski, M. M.; Smith, S. D.; Spontak, R. J. *Macromolecules* **1996**, *29*, 8862.
(14) Papadakis, C. M.; Mortensen, K.; Posselt, D. *Eur. Phys. J., B* **1998**, *4*, 325.
(15) Sakurai, S.; Irie, H.; Umeda, H.; Nomura, S.; Lee, H. H.; Kim, J. K. *Macromolecules* **1998**, *31*, 336.
(16) Jeon, H. G.; Hudson, S. D.; Ishida, H.; Smith, S. D. *Macromolecules* **1999**, *32*, 1803.
(17) Court, F.; Hashimoto, T. *Macromolecules* **2001**, *34*, 2536.
(18) Yamaguchi, D.; Hashimoto, T. *Macromolecules* **2001**, *34*, 6495.
(19) Mayes, A. M.; Russell, T. P.; Deline, V. R.; Satija, S. K.; Majkrzak, C. F. *Macromolecules* **1994**, *27*, 7447.
(20) Koneripalli, N.; Levicky, R.; Bates, F. S.; Matsen, M. W.; Satija, S. K.; Ankner, J.; Kaiser, H. *Macromolecules* **1998**, *31*, 3498.
(21) Huang, E.; Mansky, P.; Russell, T. P.; Harrison, C.; Chaikin, P. M.; Register, R. A.; Hawker, C. J. *Macromolecules* **2000**, *33*, 80.
(22) Hasegawa, H.; Hashimoto, T. *Macromolecules* **1985**, *18*, 589.
(23) Fredrickson, G. H. *Macromolecules* **1987**, *20*, 2535.
(24) Hankee, C.; Thomas, E. L.; Fetters, L. J. *J. Mater. Sci.* **1988**, *23*, 1685.
(25) Coulon, G.; Deline, V. R.; Russell, T. P.; Green, P. F. *Macromolecules* **1989**, *22*, 2581.
(26) Anastasiadis, S. H.; Russell, T. P.; Satija, S. K.; Majkrzak, C. F. *Phys. Rev. Lett.* **1989**, *62*, 1852.
(27) Mansky, P.; Liu, Y.; Huang, E.; Russell, T. P.; Hawker, C. *Science* **1997**, *275*, 1458.
(28) Morkved, T. L.; Lu, M.; Urbas, A. M.; Enrichs, E. E.; Jaeger, H. M.; Mansky, P.; Russell, T. P. *Science* **1996**, *273*, 931.
(29) Thurn-Albrecht, T.; DeRouchey, T.; Russell, T. P.; Jaeger, H. M. *Macromolecules* **2000**, *33*, 3250.
(30) Yang, X. M.; Peters, R. D.; Nealey, P. F.; Solak, H. H.; Cerrina, F. *Macromolecules* **2000**, *33*, 9575.
(31) Rockford, L.; Liu, Y.; Mansky, P.; Russell, T. P.; Yoon, M.; Mochrie, S. G. J. *Phys. Rev. Lett.* **1999**, *82*, 2602.
(32) Segalman, R. A.; Yokoyama, H.; Kramer, E. J. *Adv. Mater.* **2001**, *13*, 1152.
(33) Kim, G.; Libera, M. *Macromolecules* **1998**, *31*, 2569.
(34) Fukunage, K.; Elbs, H.; Magerle, R.; Krausch, G. *Macromolecules* **2000**, *33*, 947.
(35) Elbs, H.; Drummer, C.; Abetz, V.; Krausch, G. *Macromolecules* **2002**, *35*, 5570.
(36) Kim, S. H.; Misner, M. J.; Xu, T.; Kimura, M.; Russell, T. P. *Adv. Mater.* **2004**, *16*, 226.
(37) Spatz, J. P.; Roescher, A.; Sheiko, S.; Krausch, G.; Möller, M. *Adv. Mater.* **1995**, *7*, 731.
(38) Meiners, J. C.; Elbs, H.; Ritzi, A.; Mlynek, J.; Krausch, G. *J. Appl. Phys.* **1996**, *80*, 2224.
(39) Li, Z.; Zhao, W.; Rafailovich, M. H.; Sokolov, J.; Khougaz, K.; Lennox, B.; Eisenberg, A.; Krausch, G. *J. Am. Chem. Soc.* **1996**, *118*, 10892.
(40) Sohn, B.-H.; Yoo, S.-I.; Seo, B.-W.; Yun, S.-H.; Park, S.-M. *J. Am. Chem. Soc.* **2001**, *123*, 12734.
(41) Chen, Y.; Huang, H.; Hu, Z.; He, T. *Langmuir* **2004**, *20*, 3805.
(42) Sakurai, S.; Umeda, H.; Yoshida, A.; Nomura, S. *Macromolecules* **1997**, *30*, 7614.
(43) Hasegawa, H.; Hashimoto, T. In *Comprehensive Polymer Science, Second Supplement*; Aggarwal, S. L., Russo, S., Eds.; Pergamon: Oxford, England, 1996; p 497.
(44) Birshtein, T. M.; Lyatskaya, Yu. V.; Zhulina, E. B. *Polymer* **1992**, *33*, 2750.
(45) Carvalho, B. L.; Thomas, E. L. *Phys. Rev. Lett.* **1994**, *73*, 3321.
(46) Xuan, Y.; Peng, J.; Cui, L.; Wang, H.; Li, B.; Han, Y. *Macromolecules* **2004**, *37*, 7301.
(47) David, J. L.; Gido, S. P.; Hong, K.; Zhou, J.; Mays, J. W.; Tan, N. B. *Macromolecules* **1999**, *32*, 3216.
(48) Takahashi, K.; Hasegawa, H.; Hashimoto, T.; Bellas, V.; Iatrou, H.; Hadjichristidis, N. *Macromolecules* **2002**, *35*, 4859.
(49) Zhulina, E. B.; Lyatskaya, Y. V.; Birshtein, T. M. *Polymer* **1992**, *33*, 332.
(50) Lyatskaya, J. V.; Zhulina, E. B.; Birshtein, T. M. *Polymer* **1992**, *33*, 343.